TITLE

The width of the frequency channels determines stimulus-specific adaptation in the inferior colliculus of the rat

AUTHORS

Xin Wang[1*‡], Daniel Duque[1*] and Manuel S. Malmierca[1,2†]

ADDRESSES

[1] Auditory Neurophysiology Unit, Laboratory for the Neurobiology of Hearing, Institute of Neuroscience of Castilla y León, University of Salamanca, Salamanca 37007, Spain.

[2] Department of Cell Biology and Pathology, Faculty of Medicine, University of Salamanca, Campus Miguel de Unamuno, 37007, Salamanca, Spain.

[*] these authors contributed equally to this work

ADDITIONAL INFORMATION

Running title: **Frequency channels determines SSA**

Key words: **Auditory, SSA**

Number of pages: **34;** Number of figures: **9;** Number of tables: **1**

Abstract number of words: **245**

Introduction number of words: **560**

Discussion number of words: **1585**

Section: **systems/circuitry**

[†] Correspondence should be sent to:

Manuel S. Malmierca

Institute of Neuroscience of Castilla y León, University of Salamanca

C/ Pintor Fernando Gallego, 1

37007 Salamanca, Spain

msm@usal.es Phone: +34 923294500, ext. 5333 Fax: +34 923294750

[‡] Current address: College of Life Sciences and Hubei Key Laboratory of Genetic Regulation and Integrative Biology, Central China Normal University, Wuhan 430079, China

Author contributions

The experiments were performed in the Laboratory for the Neurobiology of Hearing, Institute of Neuroscience of Castilla y León, University of Salamanca, Salamanca, Spain. The contribution of each author to the following aspects of the study is as stated: (1) collection of data: X.W.; (2) conception and design of experiments: D.D., M.S.M.; (3) analysis and interpretation of data: X.W., D.D. and M.S.M.; (4) writing the paper: D.D. and M.S.M. All authors approved the final version of the manuscript.

Acknowledgements

We are most grateful to Dr. Eric Young for his critical and valuable comments on a previous version of this manuscript. We also thank Mr. Javier Nieto for his help and assistance in the analysis of the data. Financial support was provided by the Spanish MINECO (BFU2013-43608-P), to M.S.M. D.D. held a fellowship from the Spanish MEC (BES-2010-035649). X.W. held a fellowship from the National Natural Science Foundation of China (NNSFC-31000493). The funders had no role in study design, data collection and analysis, decision to publish, or preparation of the manuscript.

ABSTRACT

For years, electrophysiological, psychophysical and electroencephalographic studies have tried to disentangle the neuronal basis for intensity coding and intensity deviant detection. Psychophysical forward masking experiments have repeatedly shown how a higher intensity sound masks the subsequent low intensity sound, but electroencephalographic mismatch negativity experiments have proved that pre-attentive deviant detection can be elicited with low intensity deviants sounds. Here we did extracellular single-unit recording in the inferior colliculus (IC) of the anesthetized rat to test if there is stimulus-specific adaptation (SSA) for intensity deviants. We used the oddball paradigm to evaluate SSA for frequency, intensity and double deviants for frequency and intensity. Thus, if we considered two sounds of the same frequency where the low intensity sound presented a low probability of appearance, two scenarios could arise: 1) neurons adjust to stimulus statistics by changing the dynamic range to the high intensity sound or 2) SSA exists for intensity sounds and the neuron presents an enhanced response for the low intensity deviant sound. Our results demonstrate that there is no SSA for purely intensity deviant sounds in the IC, but the across-adaptation data analysis show that SSA can be found for double deviants whenever the high intensity standard present a frequency that is outside the frequency channels that code for the deviant sound. Moreover, those frequency channels broaden at higher intensities and are clearly narrower for neurons that show high levels of SSA, strongly suggesting that the frequency-channel theory is explaining SSA in the IC.

INTRODUCTION

While neuronal systems seem to follow an efficient coding strategy to properly respond the most common inputs (Wark et al., 2007), repetition in the brain usually implies adaptive processes (Grill-Spector et al., 2006). The range of intensities and frequencies that an animal can perceive is enormous and environmental changes need to be assessed rapidly and accurately. The auditory system needs to adjust its response to the stimulus statistics (Dean et al., 2005; Watkins and Barbour 2008; Wen et al., 2009; Dahmen et al., 2010; Rabinowitz et al., 2011), while the response to the less common sounds (deviants) cannot be neglected and usually present an enriched response (stimulus-specific adaptation; SSA: Ulanovsky et al., 2003; Malmierca et al., 2009). This issue has been recently discussed by two recent studies (Herrmann et al., 2014; Simpson et al., 2014).

Most studies on SSA have been realized with frequency deviant sounds (Nelken 2014), while the investigation about dynamic range adaptation has been basically performed with intensity distributions (Dean et al., 2005; 2008; Watkins and Barbour 2008; 2011; Wen et al., 2009; 2012). Beyond the frequency SSA, some investigators try to evoke such process by a plethora of features including intensity (Ulanovsky et al., 2003; Reches and Gutfreund, 2008; Farley et al., 2010), interaural differences (Reches and Gutfreund, 2008; Xu et al., 2014) and duration (Farley et al., 2010), but the existing data for intensity SSA is controversial and inconclusive. Those studies disagree regarding the response to a low intensity deviant sound embedded in a background of loud sounds. This issue is important for two reasons. It is well known that 1) a high intensity sound mask the subsequent low intensity sound (forward masking/suppression; Calford and Sample, 1995; Brosch and Schreiner, 1997) and 2) SSA is assumed to lie upstream the generation of mismatch negativity (MMN; Escera and Malmierca, 2013) and such auditory evoked potential can be elicited with low intensity deviants sounds (Jacobsen et al., 2003; Althen et al., 2011). Intriguingly, the adjustment of the neuronal response to sound intensity statistics will reduce the response to low intensity sounds if the most common sound has a higher intensity (Dean et al., 2005). But, at least in the auditory cortex, some neurons are able to preserve a delicate sensitivity to low intensity sounds (Watkins and Barbour, 2008). Therefore, SSA for low intensity deviant sounds could be evoked, even when the high intensity sound had the same frequency than the low intensity one.

We recorded extracellular single-unit IC responses in the anesthetized rat to test if there is SSA for intensity deviants. We calculate the frequency response area (FRA) for each neuron and tested the oddball paradigm for a fixed low intensity deviant sound but repeatedly varying both the frequency and the intensity of the high intensity standard sound. We also used the novel *rapid adaptation paradigm* to characterize the shape and width of the frequency channels that code for the low intensity deviant sound. Our results demonstrate that there is no SSA for purely intensity deviant sounds in the IC, and the analysis of the across-adaptation elicited by the double deviants for frequency and intensity show that SSA can be generated if and when the high intensity standard is outside the frequency channels that code for the low intensity deviant sound. This experiments reinforced the idea that SSA is a feature dependent on input-specific adaptation mechanisms.

67 **METHODS**

68 *Surgical procedures.* Experiments were performed on 37 adult pigmented female rats
69 (*Rattus norvergicus*, Long-Evans) with body weights between 150 and 260 g. All
70 experimental procedures were carried out at the University of Salamanca with the
71 approval of, and using methods conforming to the standards of, the University of
72 Salamanca Animal Care Committee. Anesthesia was induced (1.5 g/kg, i.p., 20%
73 solution) and maintained (0.5 g/kg, i.p. given as needed) with urethane. Urethane was
74 chosen as an anesthetic because its effects on multiple aspects of neural activity,
75 including inhibition and spontaneous firing, are known to be less than those of
76 barbiturates and other anesthetic drugs (Hara and Harris, 2002). The respiration was
77 maintained artificially (SAR-830/P Ventilator) monitoring the end-tidal CO_2 level
78 (CapStar-100). For this purpose, the trachea was cannulated and atropine sulfate (0.05
79 mg/kg, s.c.) was administered to reduce bronchial secretions. Details of surgical
80 procedures have been described previously (Pérez-González et al., 2005; Malmierca et
81 al., 2009). Body temperature was maintained at 38±1°C by means of a heating blanket.
82 The animal was placed in a stereotaxic frame in which the ear bars were replaced by
83 hollow speculae that accommodated a sound delivery system, inside a sound-sealed
84 room. An incision was made in the scalp along the midline, and the skin was reflected
85 laterally before a craniotomy was performed to expose the cerebral cortex overlaying
86 the left IC.

87 *Electrophysiological recording.* Extracellular single unit responses were recorded
88 using a tungsten electrode (1–2 MΩ, Merrill and Ainsworth, 1972) lowered through the
89 cortex by means of a piezoelectric microdrive (Burleigh 6000 ULN). Neuron location
90 in the IC was based on stereotaxic coordinates, physiological criteria of tonotopicity
91 and response properties (Malmierca et al., 2003; Hernandez et al., 2005) and confirmed
92 histologically afterwards. Acoustic stimuli were delivered through a sealed acoustic
93 system using two electrostatic loudspeakers (TDT-EC1: Tucker Davis Technologies)
94 driven by two TDT-ED1 modules. The stimuli were presented contralaterally to the
95 recording side; search stimuli were pure tones or noise bursts monaurally delivered
96 under computer control using TDT System II hardware and custom software (Faure et
97 al., 2003; Pérez-González et al., 2005; Malmierca et al., 2009). The output of the system
98 at each ear was calibrated *in situ* using a ¼" condenser microphone (model 4136, Brüel
99 & Kjær) and a dynamic signal analyzer (Photon+, Brüel & Kjær). The maximum output

of the TDT system was flat from 0.3 to 5 kHz (~100±7 dB SPL) and from 5 to 40 kHz (~90±5 dB SPL). The highest frequency produced by this system was limited to 40 kHz. The second and third harmonic components in the signal were ≥40 dB below the level of the fundamental frequency at the highest output level (Malmierca et al., 2009). Action potentials were recorded with a BIOAMP amplifier (TDT), the 10x output of which was further amplified and bandpass-filtered (TDT PC1; f_c, 500 Hz and 3 kHz) before passing through a spike discriminator (TDT SD1). Spike times were logged with a resolution of ≈150 μs on a computer by feeding the output of the spike discriminator into an event timer (TDT ET1) synchronized to a timing generator (TDT TG6). Stimulus generation and on-line data visualization were controlled with custom software. Spike times were displayed as dot rasters sorted by the acoustic parameter varied during testing.

From each isolated neuron, the approximate frequency tuning was audiovisually determined by presenting pure tones lasting 75 ms with a 5 ms rise/fall time (Hernandez et al., 2005). We obtained the monaural frequency response area (FRA), the combination of frequencies and intensities capable of evoking a response, as an estimation of the neuronal receptive field. For that, we presented multiple combinations of frequency and intensity using an automated procedure with 5 stimulus repetitions at each frequency (from 0.5 to 40 kHz, in 25 logarithmic steps, presented randomly) and intensity (10 dB steps, presented from lower to higher intensities). The spike counts evoked at each combination of frequency and intensity were plotted using MATLAB®.

Stimulus presentation paradigms. The representation of the FRA allowed us to choose different pairs of tones within the auditory field of the neuron. First of all, we set a pair of frequencies (f_1 and f_2) that elicited a similar firing rate at 10-20 dB above the best frequency threshold. Then, stimuli were presented in an oddball paradigm similar to that used to record mismatch negativity responses in human (Näätänen, 1992) and animal studies (*e.g.*, Ulanovsky et al., 2003; Malmierca et al., 2009). Briefly, a train of 400 stimuli containing both frequencies f_1 and f_2 was presented under the oddball paradigm: one frequency (f_1) was presented as the standard stimuli while, interspersed randomly among the standards, the deviant stimuli were presented at the second frequency (f_2). After obtaining one data set, the relative probabilities of the two stimuli were reversed, with f_2 as the standard and f_1 as the deviant. At the regular frequency deviant oddball paradigm used in this manuscript, the frequency contrast remained

constant at Δf=0.10 (0.141 octaves); where $\Delta f = (f_2 - f_1) / (f_2 \times f_1)^{1/2}$. The stimuli were always presented at a repetition rate of 4 Hz (inter-stimulus interval, ISI=250 ms) and the probability of appearance of the deviant stimulus was fixed at 10%. This condition has previously shown to evoke high neuronal levels of SSA in the IC (Malmierca et al., 2009; Duque et al., 2012). Thus, we used it to calculate an overall level of frequency-deviant SSA of each neuron. In order to have a more reliable analysis of the adaptation phenomenon, we fixed one of the frequencies used before (generally f_1) and calculated the response of that frequency in a deviant alone protocol, where we tested an oddball paradigm but the standard stimuli is replaced by silence. Under that circumstance, the response to the deviant stimuli is the maximum possible for a given frequency because it is not affected by any kind of adaptation.

Besides the calculation of the level of SSA for frequency deviants, we used the oddball paradigm to characterize how different frequencies at different intensities could affect the response to a low intensity deviant sound (Figure 1A). For this reason, keeping the deviant frequency fixed, we repeated the oddball paradigm but varied the intensity contrast (Δi=10 dB, Δi=20-30 dB and Δi=40-50 dB), the frequency contrast (Δf=0, Δf=0.04 [0.057 octaves], Δf=0.10 [0.141 octaves] and Δf=0.37 [0.526 octaves]) or both. As before, after obtaining each data set the relative probabilities of the two stimuli were reversed. The analysis of the response to the deviant sound allowed us to obtain a map of the different standard sounds that affect the low intensity deviant sound. Figure 1B shows three different examples of the usage of the oddball paradigm to this purpose: 1) pure frequency deviant oddball paradigm (Δf=0.1, orange hexagon), 2) pure intensity deviant oddball paradigm (Δi=10, violet square) and 3) double deviant oddball paradigm (Δf=0.1 and Δi=10, black diamond). Hereinafter, when we speak of intensity and double deviant protocols, deviant and probe (p) will refer to the frequency fixed at the low intensity, while standard and conditioner (c) will refer to the frequency used at high intensities. When probing for SSA at different frequency- and intensity contrasts, we started to collect the data from the smaller intensity contrast (Δi=10) and we used, at least, two different frequency contrasts. Then, we tried to cover all the possible range of intensity contrasts at the same frequency contrasts used before. A complete protocol in a neuron lasted for ~90 min and allowed us to see the effect of 13 different frequencies /intensities over the probe sound (Figure 1A). In order to simplify the analysis of the data and to reduce the time of the experimental protocol, we decided to

always pick conditioner frequencies higher than the probe sound. This decision was taken because SSA levels are more evident at the high frequency range (Duque et al., 2012).

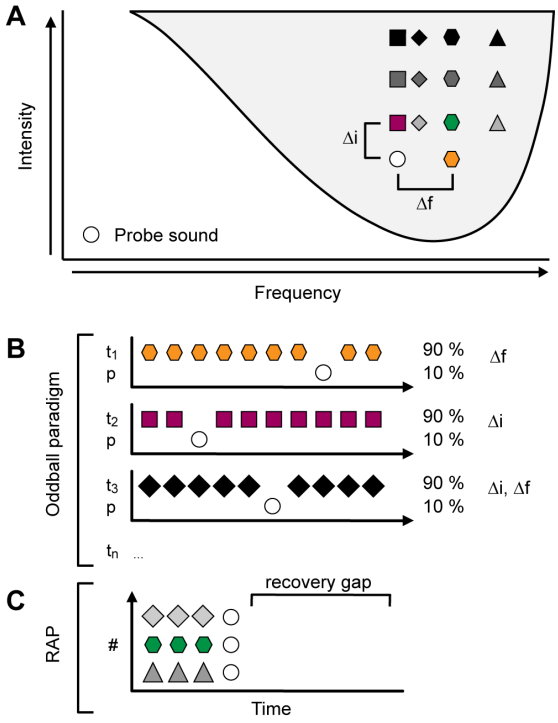

Figure 1. Experimental design. A. Schematic FRA showing the stimulation protocol of the experiments. A low intensity deviant pure tone (white circle) is fixed at the neuronal best frequency 10-20 dB over threshold. Different conditioner sounds (squares, diamonds, hexagons and triangles) at different frequency- (Δf) and intensity contrasts (Δi) are used to check the across adaptation to the low intensity sound. **B.** Oddball paradigm. Four hundred pure tone sequences with a deviant (10% prob.) and a standard sound (90% prob.) were presented. The ISI was kept constant al 250 ms. Several different pairs of frequencies arise considering the standard sound used: frequency deviant (orange hexagon); intensity deviant (violet square); double deviant (black diamond)… Low intensity deviant sound responses are analyzed to check for across adaptation. **C**. Rapid adaptation paradigm (RAP). Two thousand ms sequences with 4 tones (3 repeated high intensity standard sounds and the low intensity deviant sound; ISI=250 ms) and 1000 ms silence period (recovery gap) were presented. The whole range of frequencies and intensities used for computing the FRA is used in the RAP protocol. Reduced low intensity deviant sound responses after a determined high intensity standard sound are assumed to be due across adaptation.

Subsequently, with the aim of complete the previous oddball paradigm data with the effect of low frequency conditioners over the probe sound, we established a novel rapid adaptation paradigm (RAP, Figure 1C). The RAP merged the concepts of two tones suppression experiments (*e.g.*, Nelson et al., 2009) with the protocol to generate a FRA (see above). A sequence is generated with 1) a random tone at a determined frequency and intensity (conditioner, c) repeated three times before 2) a fixed sound (probe, p) is

presented. The stimuli were presented at a rate of 4 Hz (ISI=250 ms) and a recovery gap of 1000 ms is established after the probe sound, generating a 2000 ms sequence with 4 sounds and a 1000 ms silence period (Figure 1C. *c c c p*). If the conditioner frequency were related to the probe sound, the adaptation observed during the three-conditioner repeated tones would also adapt the probe sound. If both tones are unrelated, the response to the probe sound will be as is obtained when the probe is presented alone, unaffected by the adaptation observed during the repetition of the three-conditioner tones. Similar to the FRA, we presented 4 sequence repetitions at multiple frequencies (25 logarithmic steps, presented randomly) and intensities (10 dB steps, presented from lower to higher intensities), covering the previously generated FRA. The firing rate of the probe sound–related to the conditioner sound– was then plotted in MATLAB®. The graph obtained showed an area of frequencies and intensities within the FRA with suppressed responses. The bandwidth of the frequency channel was taken to be the frequencies where the response to the probe sound was less than (1-*criterion*) * *baseline response*. The baseline response was the mean response to the probe tone when it was preceded by conditioner tones at the lowest intensity; the criterion values was 0.4 (Scholes et al, 2011). Bandwidths at 10 and 30 dB relative to the best frequency threshold (reTh) were calculated. The ratio between the bandwidths of the frequency channel and the FRA was also computed to extract the relative width of the frequency channel.

Data analysis. Dot raster plots are used to illustrate the responses obtained to the oddball paradigm, plotting individual spikes (red dots indicate responses to the deviant; blue dots to the standard, and green to the deviant in a deviant alone protocol). Stimulus presentations are marked along the vertical axis. The responses to the standard and deviant stimuli were expressed as spikes per stimulus in a peri-stimulus time histogram (PSTH), to account for the different number of presentations in each condition. The amount of SSA was quantified in different ways. First, we calculated the common SSA index (CSI) and the frequency-specific index (SI_{f1}) from the firing rate elicited in the oddball paradigm. They were defined as $CSI = [d(f_1) + d(f_2) - s(f_1) - s(f_2)] / [d(f_1) + d(f_2) + s(f_1) + s(f_2)]$, where d(f) and s(f) are responses to each frequency f_1 or f_2 when they were the deviant (d) or standard (s) stimulus and as $SI_{f1} = [d(f_1) - s(f_1)] / [d(f_1) + s(f_1)]$, defined for the fixed frequency ($f1$). The values of these indices range from –1 to +1, being positive if the response to the deviant stimulus is greater. Both indexes are well

defined and have been used in previous studies, proving to be useful when the firing rate of the both frequencies is similar and when used for computing SSA for frequency deviants (*e.g.*, Ulanovsky et al., 2003; Malmierca et al., 2009). We also used the normalized index of adaptation (NIA) defined for deviant as NIA_{dev}= d(f_1)/ d($f_{1\text{-}alone}$) and for standard as NIA_{std}= s(f_1)/ d($f_{1\text{-}alone}$). We do not use a correction for spontaneous rate because the values are usually negligible in the urethane-anesthetized rat and mice (Duque et al., 2012; Duque and Malmierca, 2014). The NIA works with the assumption that the response to the sound in the deviant alone protocol is the maximum possible for a given frequency because is not affected by any kind of adaptation. In the NIA, responses to the standard or deviant sound are divided by the response in the deviant alone protocol, reflecting the extent to which the response to the standard or the deviant is reduced compared to the computed maximum response. NIA range from 0 to 1, being 1 if the response to the sound is maximal (*i.e.*, not adapted) and 0 if the response to the sound is totally suppressed. A Wilcoxon rank paired t-test comparing the NIA values for the standard (NIA_{std}) and the deviant (NIA_{dev}) at the same condition allows for computing SSA.

Statistical tests were performed using non-parametric tests. For comparing data from different groups, we used Mann-Whitney rank tests. For comparisons between the same data at different conditions, we used Wilcoxon rank paired t-tests. Multiple comparisons were realized with the Kruskal-Wallis test and the differences were confirmed with the Dunn's *post-hoc* analysis. All the statistical tests were considered significant when $p \leq 0.05$. Different statistical tests were noted in the paper. The analysis and figures were done using Sigmaplot 11 (Systat Software) and MATLAB® (MathWorks).

RESULTS

We recorded single unit responses from 132 well-isolated neurons in the IC of the rat, determined the basic temporal and spectral response properties of each neuron and chose a pair of frequencies within the FRA to evaluate SSA for frequency deviants under an oddball paradigm. Then, in order to test whether or not genuine SSA exists for intensity deviants, we fixed one of the frequencies used for the frequency deviant protocol and tested again the oddball paradigm but in this case for sounds that only differed by intensity. Finally, we also checked how responses to high intensity sounds affect the level of SSA of a low intensity tone. In the following, first we describe SSA responses of IC neurons for frequency and intensity deviants and then we will detail how the responses to low intensity sounds are modified by high intensity sounds.

SSA for frequency deviants

The common SSA index (CSI) was used to quantify the degree of neuronal adaptation in an oddball paradigm with a frequency contrast (Δf) of 0.1 and a repetition rate of 4 Hz (n=117), a condition that previous studies demonstrated to evoke high levels of SSA (Malmierca et al., 2009). CSI levels in this condition range from -0.09 to 0.99 with an average of 0.49±0.34 (mean±S.D.) and confirm our previous data (Malmierca et al., 2009, Duque et al., 2012; Ayala et al., 2013). A CSI cut-off value of +0.18 was defined as significant SSA based on previous data (*e.g.* Antunes et al., 2010). Using this criterion, 81 neurons (69%) in our sample showed significant SSA, while the remaining 36 (31%) did not. We also quantified the degree of SSA using the frequency-specific SSA index (SI). The scatter plot in figure 2A shows the SI values for each frequency used in the oddball paradigm (SI_{f1} vs. SI_{f2}). As expected (Malmierca et al., 2009; Duque et al., 2012, 2014; Ayala et al., 2013), the majority of values are located in the upper 'right' quadrant, and therefore they show significant SSA.

SSA for intensity deviants

Next, we fixed one of the two frequencies used before (generally *f1*) and tested the neuron again using the oddball paradigm. In this case the second sound had the same frequency (Δf=0) but different intensity (Δi=10 dB). As a control, we also tested the oddball paradigm while varying both the frequency and the intensity, establishing a double deviant protocol (Δf=0.1; Δi=10 dB, Figure 1A). Hereinafter, when we speak

of intensity and double deviant protocols, *f1* and probe (p) will refer the frequency fixed at the low intensity. To facilitate comparisons, the colors of the conditions in the scatter plots shown in Figure 2 are the same as in Figure 1: the open white circle is the fixed probe frequency (*f1*, p) and the 3 different colors represent the 3 different standard frequencies (conditioner, c) at the 3 different oddball paradigm protocols. Figure 2B shows the scatter plot for the SI values in the double deviant condition, *i.e.*, when we varied frequency and intensity in concert (n=97; the low intensity probe sound [*f1*] is presented in the x-axis). The levels of CSI recorded in this condition range from -0.04 to 0.99, with a mean value of 0.51±0.33 (mean±S.D.). The distribution of the dots in Figure 2A and 2B is almost identical, as the majority of values are located in the upper 'right' quadrant, demonstrating unambiguously the presence of genuine SSA, meaning adaptation for both frequencies as standards. Nevertheless, a few SI values for the low intensity sound (SI_{f1}: 6 cases, 6%) lie at SI = -1, meaning that there is no response at all for the low intensity deviant sound.

By contrast, Figure 2C shows the scatter plot for the SI values when we tested an oddball paradigm with two sounds of the same frequency that differed in intensity only (Δi=10 dB, n=117; the low intensity sound [*f1*] is presented in the x-axis). The CSI values range from -0.04 to 0.92 with a mean CSI value of 0.35±0.29 (mean±S.D.). Since the CSI values for the intensity deviant condition were lower than the values obtained before for the frequency deviant and the control condition, we run a Kruskall-Wallis ANOVA on Ranks test to check if there were some differences between the conditions ($H=16.70$; $p<0.001$). Dunn's method *post hoc* test confirmed that the CSI values in the intensity deviant condition were smaller than in the frequency and the double deviant condition ($Q=3.72$ and $Q=3.26$, respectively; $p<0.01$ in both cases). Furthermore, a simple visual inspection of the values in Figure 2A and 2B show a different distribution to that at Figure 2C, because of the SI values obtained in the oddball paradigm for the low intensity sounds (SI_{f1}). Indeed, a majority of the values (95 out of 117 neurons analyzed; 81.2%) were found in the upper 'left' quadrant and had a negative SI_{f1} value. Moreover, 44 values (37.8%) are unresponsive to low intensity sounds, show a -1 SI_{f1} and lay on the left y-axis. Only 4 neurons (3.4%) presented a SI_{f1} value larger than 0.18 (the cut-off value used for significant SSA), although a detailed analysis of the SI_{f1} values show that they were not different from 0 and, therefore, we considered the values outliers (bootstrap over 1000 randomizations).

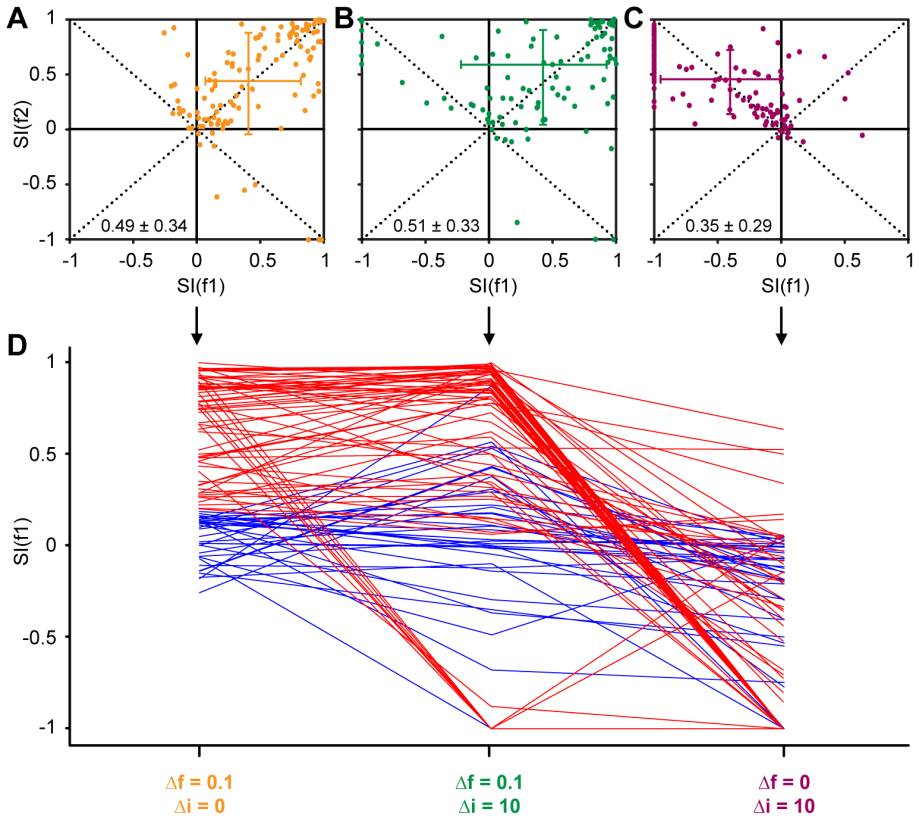

Figure 2. IC neurons do not show pure intensity deviant SSA. A. Scatter plot of the SI(*f1*) versus SI(*f2*) for the frequency deviant pairs of frequencies analyzed at a Δ*f*=0.1. The cross indicates the median and the 25th-75th interquartile range for each axis. Each neuron was tested using different combinations of parameters and may be represented in additional panels. Median CSI value is shown at the bottom of the plot. **B.** Scatter plot of the SI(*f1*) versus SI(*f2*) for the double deviant condition (mixed frequency and intensity deviant pairs of frequencies) analyzed at a Δ*f*=0.1 and Δ*i*=10. SI(*f1*): Low intensity probe SI. SI(*f2*): High intensity conditioner SI.**C.** Scatter plot of the SI(*f1*) versus SI(*f2*) for the intensity deviant pairs of frequencies analyzed at a Δ*i*=10. SI(*f1*): Low intensity probe SI. SI(*f2*): High intensity conditioner SI. **D.** Changes in SI(*f1*) values for each neuron at the three previous conditions: pure frequency deviant (left column), double deviant (middle column) and pure intensity deviant (right column). The values are sorted for neurons with low- (blue lines) and high SSA (red lines) for frequency deviants. Note the drop in intensity SSA levels for neurons with good sensitivity for frequency SSA. Neurons with low frequency SSA sensitivity present also low levels for intensity SSA.

Responses to the high intensity tones adapt the responses to low intensity sounds

If we only analyze the SI values for the frequency fixed (SI_{f1}, Figure 2D) rather than the CSI, the results indicate in reality an apparent SSA for intensity deviant sounds. At first sight, we can observe two clearly differentiated populations. The first one, which showed SI_{f1} values for frequency deviants larger than +0.18 (red lines, significant SSA levels), generally presented similar values in the frequency deviant condition (Figure 2D, left column) and the double deviant condition (Figure 2D, middle column), but a big SI_{f1} drop when we test the oddball paradigm for the intensity deviant condition (Figure 2D, right column). As before, in several cases the SI_{f1} values are -1, indicating that there is no response to the low intensity sound. The second population showed SI_{f1} values smaller than +0.18 (Figure 2D, blue lines) and had neither SSA for frequency nor for intensity deviants, with SI_{f1} values generally close to 0 in the three different conditions. The above indicates that the 'classic CSI' metric is not appropriate to evaluate intensity deviants because it is clearly biased by the reverse condition in the oddball paradigm, where the deviant sound presents a consistent response when it has a higher intensity than the standard sound. Figure 3 shows a typical example illustrating this effect. For the dot rasters (Figure 3B-E) we only highlight the responses to the low intensity sound colored (Figure 3A, *f1*, white empty circle) in the three different conditions shown before: frequency-, double- and intensity deviant. Figure 3B shows the response to *f1* in a deviant alone protocol (green dots and lines), where the response should not be affected by adaptation and, therefore, to be maximum (see Methods).

The evaluation of the CSI for the frequency- (Figure 3C) and the double deviant condition (Figure 3D) undoubtedly embodies genuine SSA, as compared to the SI_{f1} values. But when evaluating purely intensity deviants (Figure 3E) CSI fails to represent SSA, giving values comparable to the other conditions because of the bias due to the SI_{f2} value obtained in the reverse high intensity deviant condition (grey dots). A closer inspection to the dot rasters in Figure 3E allows to see the vanishing of the response to the low intensity deviant (Figure 3E, no red dots in the bottom scatter plot) when the standard sound is louder, while the response to the high intensity deviant sound is extremely reliable because the standard has a lower intensity and it is not affecting the response to the high intensity deviant (Figure 3E, grey dots).

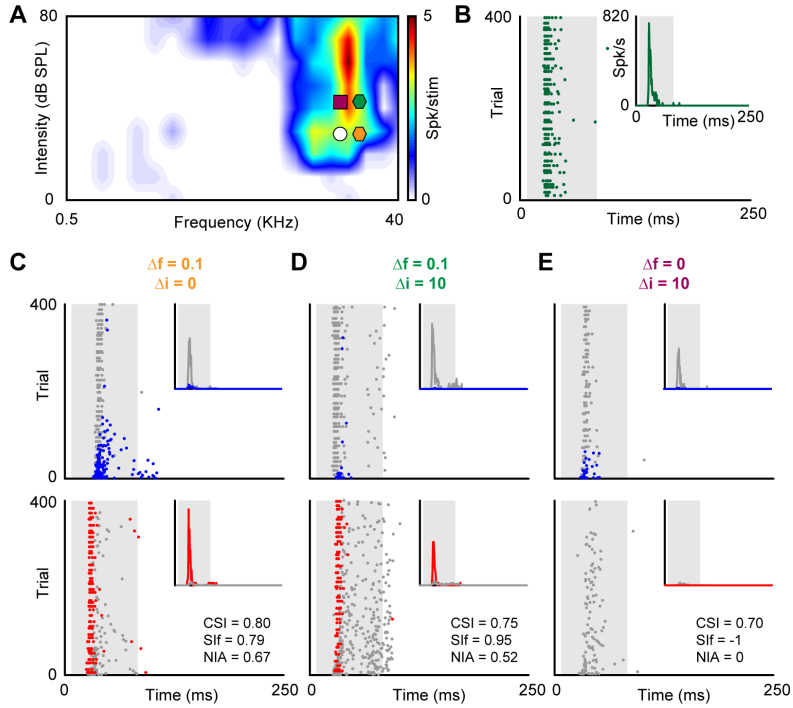

Figure 3. CSI misrepresent intensity SSA. A. FRA of an IC neuron. A low intensity sound (*f1*, white circle) and three different frequencies (Δ*f*=0.1: orange hexagon; Δ*f*=0.1 at Δ*i*=10: green hexagon; Δ*i*=10: violet square) are represented over the FRA. **B.** Dot raster plot illustrating responses of the low intensity sound in the deviant alone protocol. **C-E.** Below the FRA, dot raster plots are illustrated for the oddball paradigm with 3 three different frequencies establishing: **C.** a frequency deviant oddball paradigm, Δ*f*=0.1: orange hexagon in 3A. **D.** a double deviant oddball paradigm, Δ*f*=0.1 at Δ*i*=10: green hexagon in 3A and **E.** a intensity deviant oddball paradigm, Δ*i*=10: violet square in 3A. In the top row the response to the low intensity sound as standard (90%) are represented in blue. In the bottom row –the reverse condition– responses to the low intensity sound as deviant (10%) are represented in red. Insets represent the PSTHs for the low intensity sound as deviant (red) or standard (blue). Responses to the other frequencies are plotted in grey but are not analyzed. Shaded backgrounds indicate the duration of the stimulus. CSI, SI($_{f1}$) and NIA values obtained in each condition are shown as insets in the bottom row. Observe that the CSI value obtained do not reflect the response observed in the intensity deviant condition (red responses in **E**).

Next, we wonder if the frequency specific SI is a better index for studying SSA at the intensity domain. In some cases, when no response is present for the low intensity deviant (Figure 3E), SI$_{f1}$ works properly to evaluate intensity SSA. In other cases, a minimal response also biased the SSA levels observed by SI$_{f1}$. Figure 4 illustrates an

example where the CSI fails to reflect the neural SSA in the intensity deviant case and SI_{f1} also fails to do it in this case (Figure 4E). The consistent, although minimal, response to the low intensity deviant sound (red dots in the bottom Figure 4E) results in an exceptionally high level of SI_{f1} that reflect the responses observed in the dot rasters for the frequency- and the double deviant condition inaccurately (Figure 4C-D). Thus, in order to define and use an indicator that represents more objectively the adaptation in the intensity domain, we defined the *normalized index of adaptation* (NIA, see Methods). A simple comparison between the NIA values for the standard (NIA_{std}) and the deviant sounds (NIA_{dev}) at the same condition not only allows for a consistent SSA index, but also highlight the effect of high intensity sounds on the adaptation of the low intensity ones (Figure 3E and 4E).

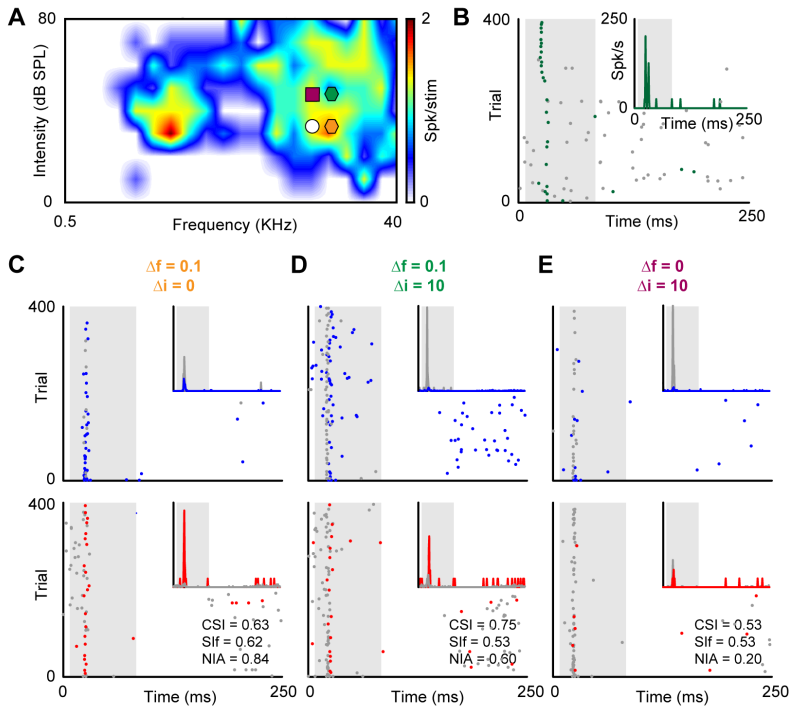

Figure 4. SI($f1$) misrepresent intensity SSA. Same conventions as in Figure 3. **A.** FRA of an IC neuron. **B.** Deviant alone responses for low intensity sound (*f1*, white circle). **C.** Frequency deviant responses for the low intensity sound (Δf=0.1: orange hexagon in 4A). **D.** Double deviant responses for the low intensity sound (Δf=0.1 at Δi=10: green hexagon in 4A). **E.** Intensity deviant responses for the low intensity sound (Δi=10: violet square in 4A). Note that the SI($f1$) value obtained do not reflect the response observed in the intensity deviant condition (red responses in **E**).

343 Next, we aimed to gain an understanding on how different frequencies (for
344 now on: conditioners, c) at different intensities affect the adaptation of the low intensity
345 sound. We used the oddball paradigm fixing one frequency (*f1*, for now on: probe, p)
346 and varying the frequency contrast (Δf=0, Δf=0.04, Δf=0.10 and Δf=0.37) and the
347 intensity contrasts (Δi=10, Δi=20-30 and Δi=40-50 dB).

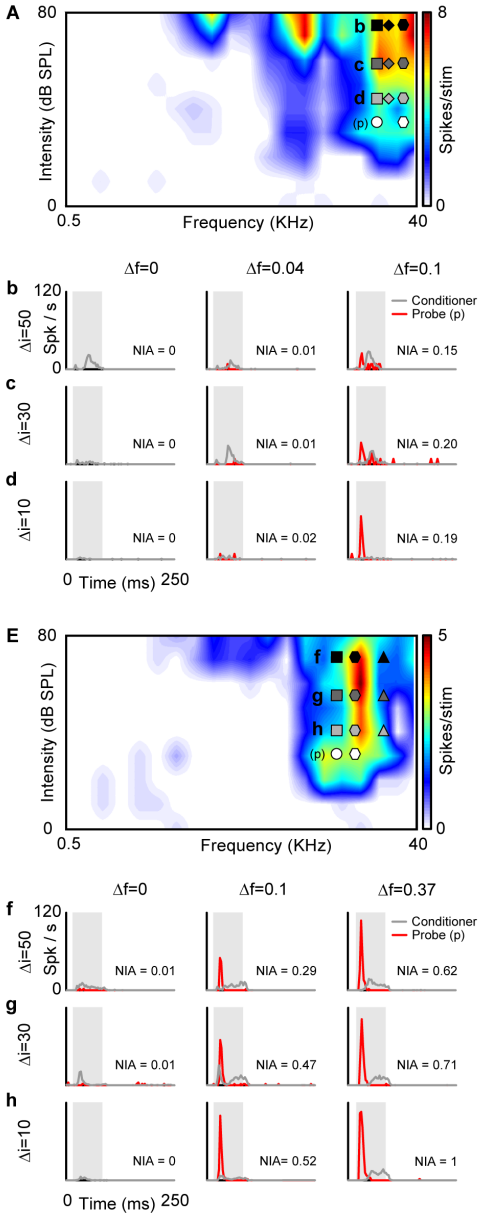

Figure 5. Two neuronal examples of intensity deviant SSA. A. FRA of an IC neuron. Probe sound (white circle, *p*) and nine different conditioner sounds covering the high frequency range of the FRA are represented over the FRA. The conditioner sounds were used at 3 frequency contrasts (Δ*f*=0, Δ*f*=0.04 and Δ*f*=0.10) with 3 intensity contrasts: **b.** Δ*i*=50 dB. **c.** Δ*i*=30 dB. **d.** Δ*i*=10 dB. **b-d.** Below the FRA, PSTHs are illustrated for the probe response in the oddball paradigm with the nine different conditioner sounds. **E.** FRA of another IC neuron. Same conventions as in **A**. Oddball paradigm was performed at 3 frequency contrasts (Δ*f*=0, Δ*f*=0.1 and Δ*f*=0.37) with 3 different intensity contrasts: **f.** Δ*i*=50 dB. **g.** Δ*i*=30 dB. **h.** Δ*i*=10 dB. **f-h.** PSTHs show the probe responses with the different conditioner sounds. Intensity deviant SSA can only be evoked if the high intensity conditioner sound differs in frequency from the probe sound.

Figure 5 shows examples of two typical neurons. In both cases we observed the lack of response to the low intensity sound as deviant when the conditioner sound is the same frequency at a higher intensity (Figure 5b-d and 5f-h, left column, NIA≈0). In general, at low frequency contrasts we observed the same trend (Figure 5b-d, Δf=0.04: middle column, NIA≈0), but the responses to the low intensity deviant sounds usually resulted in larger NIA values at higher frequency contrasts (Figure 5f-h, middle and right column, Δf=0.1 and Δf=0.37 respectively). When the intensity contrast is larger (Δi=40-50 dB, Figure 5b and 5f), the NIA levels usually decreased compared with the NIA levels observed at low intensity contrasts. This findings suggests that the frequency channel that codes the response for the low intensity sound gets broader as sounds are louder, giving the possibility to high intensity sounds at large frequency contrasts to affect the adaptation of the low intensity sound.

In order to check if this notion is true, we divided the data in two groups: neurons with significant SSA at the regular frequency-deviant oddball condition (Figure 6A and 6B; CSI≥0.18) and neurons that lack SSA at the same condition (Figure 6C and 6D; CSI<0.18). For both populations we analyzed 1) the SSA levels by comparing the NIA values for the standard and the deviant sounds (Figure 6A and 6C) and 2) the latency difference between the response to the standard and that of the deviant sound (Figure 6B and 6D). When we analyzed the neurons with high frequency-SSA levels, we observed –as expected– that the NIA_{dev} value in that condition was significantly higher level than the NIA_{std} (Figure 6A, first column; NIA_{std}: blue median, NIA_{dev}: red median; Wilcoxon paired t-test, Z=7.9, $p<0.001$, to simplify the chart NIA_{std} levels at other conditions are not shown). When we analyzed the NIA_{dev} at a Δf=0, the levels are statistically different than the NIA_{std} at the three Δi, but in this condition the response to the standard is always larger than the response to the deviant (Wilcoxon paired t-test, low Δi Z=-5.2, mid Δi Z=-5.0 and large Δi Z=-2.7, $p<0.001$ in the three cases). This result implies that the response to a high intensity tone clearly adapts (and sometimes totally suppresses) the response to the same tone at a low intensity. If we slightly change the frequency of the high intensity conditioner (Δf=0.04), the responses to the low intensity deviant sound were greatly reduced, but they did not present significant differences with the response to the low intensity standard response (Wilcoxon paired t-test, $p>0.1$ in the three cases). By contrast, at a Δf=0.1 the neurons recovered the differential responsiveness observed in the frequency deviant oddball

condition (NIA_{dev}>NIA_{std}: Wilcoxon paired t-test, low Δi Z=7.1, mid Δi Z=5.8 and large Δi Z=4.9, p<0.001 in the three cases). This trend was maintained and even enhanced at a Δf=0.37 (Wilcoxon paired t-test, low Δi Z=4.6, mid Δi Z=4.1 and large Δi Z=2.9, p<0.001 in the three conditions).

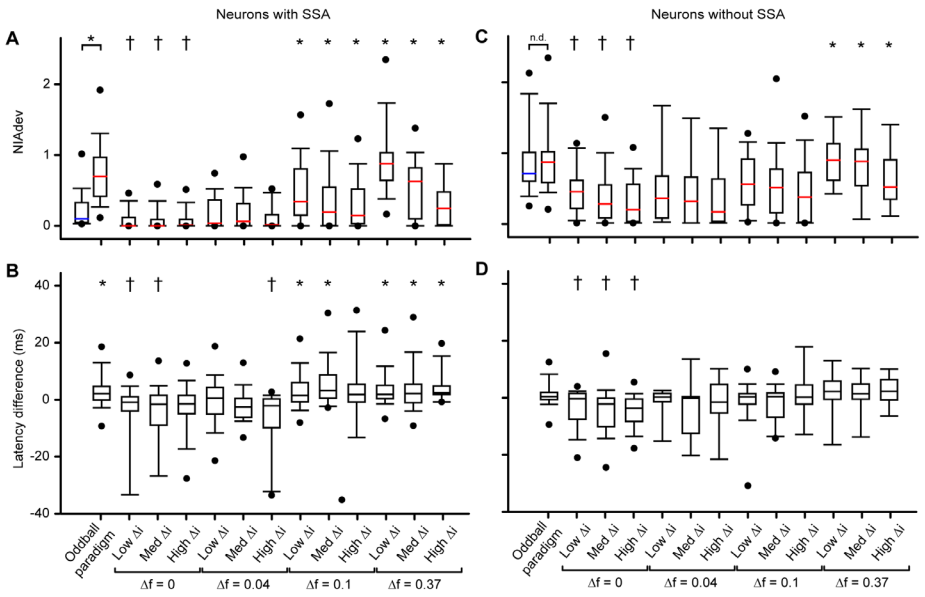

Figure 6. Frequency channels are narrow in neurons with frequency deviant SSA. **A.** Box plot illustrating the average NIA_{dev} values of the probe sound for neurons with frequency deviant SSA. Different conditioners are presented at different frequency (Δ*f*=0, Δ*f*=0.04, Δ*f*=0.1 and Δ*f*=0.37) and intensity contrasts (Δ*i*=10, Δ*i*=20-30 and Δ*i*=40-50). NIA_{std} values are not plotted to simplify the plot. Asterisks (*) show statistical differences (NIA_{dev} > NIA_{std}). Crosses (†) show significant differences in the other direction (NIA_{dev} < NIA_{std}). Higher responses to the low intensity deviant probe sound can be obtained when Δ*f*≥0.1. **B.** Box plot illustrating the latency difference of the probe sound (standard – deviant) at the same conditions presented in **A**. The changes in latency to the probe sound mimic the changes in the NIA_{dev} level. **C.** Box plot illustrating the average NIA_{dev} values of the probe sound for neurons without frequency deviant SSA. Same conventions as in **A**. **D.** Box plot illustrating the latency difference of the probe sound (standard – deviant) at the same conditions presented in **C**. Note that higher responses to the low intensity deviant probe sound can only be obtained when Δ*f*≥0.37. The frequency channel that codes for the probe sounds seem to be wider in the neurons without frequency deviant SSA.

Next, we analyzed the latency difference (Figure 6B), as a difference in latency between the standard and the deviant responses is a sign of a differential input processing of the sounds. As usual, the latency difference for the frequency deviant oddball paradigm was positive, being the latency for the standard response larger than the latency for the same sound as deviant (one sample Wilcoxon test, $t=3.3$, $p=0.001$). When we analyzed the latency data at a $\Delta f=0$ the resultant latency difference is negative regardless of the Δi, being the latency for the deviant response larger than the latency for the standard sound (one sample Wilcoxon test; low Δi $t=-2.3$, mid Δi $Z=-2.1$ and large Δi $Z=-1.9$; $p=0.02$, $p=0.04$ and $p=0.06$, respectively). Note that, to avoid data bias the latency difference was not calculated if the neuron showed no response to the low intensity deviant sound, but the data shows that the processing of the high intensity sound is producing a delay in the response to the low intensity sound. A similar trend was observed again at a $\Delta f=0.04$ but, similarly to what we saw with the firing rate adaptation, if the high intensity sound was placed outside the theoretical frequency channel ($\Delta f=0.1$ or $\Delta f=0.37$), the processing of both sounds was again independent, and the latency difference recovered the positive values observed in the frequency deviant oddball paradigm (*e.g.* at $\Delta f=0.37$: one sample Wilcoxon test; low Δi $t=2.6$, mid Δi $Z=2.1$ and large Δi $Z=3.4$; $p=0.01$, $p=0.05$ and $p=0.003$, respectively).

When we analyzed the data for the neurons with non-significant SSA ($CSI<0.18$) the trend noted for the SSA neurons was preserved, although some important differences emerged. First of all, as expected, the overall adaptation is greatly reduced compared with the neurons with significant SSA (Figure 6A-C). But, as for the neurons with significant SSA, the NIA_{dev} and NIA_{std} levels at a $\Delta f=0$ are different at the three Δi, presenting always a response to the standard tone higher than the response to the deviant tone (Wilcoxon paired t-test, low Δi $Z=-3.9$, mid Δi $Z=-4.3$ and large Δi $Z=-3.2$, $p\leq0.001$ in the three cases). However, the main difference was related to the frequency contrast and the recovery of the deviant response to the levels observed in the frequency deviant oddball paradigm: non-significant SSA neurons did not show differences in the NIA levels between the responses to the same tone as deviant or standard at either $\Delta f=0.04$ or $\Delta f=0.1$ (Wilcoxon paired t-test; $p>0.2$ in all the cases, data not shown) and the response to the deviant sound was only higher than the response to the standard tone at a $\Delta f=0.37$ (Wilcoxon paired t-test, low Δi $Z=3.0$, mid Δi $Z=2.0$ and large Δi $Z=2.0$, $p<0.05$ in the three conditions). The above implies that the neurons

lacking SSA possess: 1) a broader frequency channel than SSA neurons and 2) less ability to adapt to sounds in general. This notion is supported by the latency data analysis. As for the SSA neurons, the analysis of the latency data at a Δf=0 resulted in a negative latency difference regardless of the Δi, being the latency for the deviant response larger than the latency for the standard sound (one sample Wilcoxon test; low Δi t=-3.7, mid Δi Z=-4.4 and large Δi Z=-4.7; $p<0.05$ in the three cases). Again, the processing of the high intensity sound affects the processing of the low intensity sound. Surprisingly, the latency difference never recovered the positive values observed in the regular frequency deviant oddball paradigm (one sample Wilcoxon test; $p>0.1$ in all the cases at Δf=0.04, Δf=0.1 and Δf=0.37). Thus, although the response to the high intensity sound at a large frequency contrast (Δf=0.37) did not adapt the low intensity sound (Figure 6C), the lack of latency difference between the standard and the deviant sounds imply a certain degree of across-frequency adaptation (Figure 6D).

To evaluate the across-frequency adaptation from high- to low intensities, we analyzed the temporal dynamics of adaptation of the standard sound at three different conditions (Figure 7A): with frequency- (Δf=0.1; orange), double- (Δf=0.1, Δi=10; green) and intensity deviant sounds (Δi =10; burgundy). Then, we fitted the responses with a double exponential function (Figure 7B) defined as $f(t) = A_{stst} + A_r \cdot e^{-t/\tau(r)} + A_s \cdot e^{-t/\tau(s)}$ (*e.g.* Pérez-González et al., 2012). The response probability to the standard stimulus is rapidly reduced after the first stimulus trials in the three cases, but the speed of the decay is faster if the deviant sound is presented at higher intensities (Figure 7A and Table 1, $\tau(r)_{\text{freq. dev.}} = 7.86$; $\tau(r)_{\text{double dev.}} = 0.85$; $\tau(r)_{\text{int. dev.}} = 0.78$). If a high intensity sound is embedded within a stream of low intensity sounds, the neuron favors the response of the high intensity sound and adapt the low intensity sound, if and when the high intensity conditioner is within the frequency channel of the probe sound. Note that the asymptote of the curve (A_{stst}) is similar in the three cases (Table 1), demonstrating a common plateau at the end of the adaptation process. In other words, high intensity sounds increase the speed of adaptation, but do not alter the degree of adaptation.

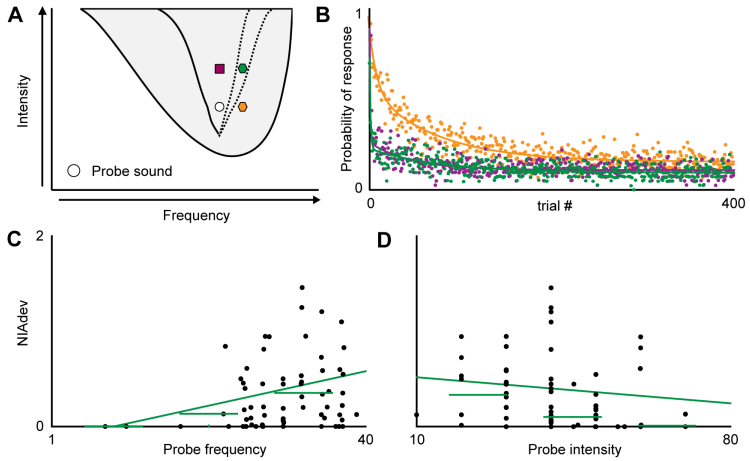

Figure 7. Frequency channel properties. A. Schematic FRA showing a probe sound (white circle) and the three conditioner sounds (orange hexagon: Δf=0.1, green hexagon: Δf=0.1 at Δi=30 and violet square: Δi=30) used to compute the time course of adaptation at different conditions. **B.** Probability of response to the standard stimulus at the three conditions stated in **A**. The higher intensity conditioner allows for a rapid adaptation regardless of the frequency of the conditioner. **C.** Dispersion chart of the NIA_{dev} values against the probe frequency. The higher the frequency, the narrower the frequency channel. **C.** Dispersion chart of the NIA_{dev} values versus the probe intensity. The higher the intensity, the wider the frequency channel.

Table 1. Double exponential coefficients at different conditions (mean ± 95% c.i.). Superimposition with the 95% c.i. in the control condition indicates that there are no significant differences between the groups. Asterisk (*) shows statistical differences.

Condition (r^2)	Fast component		Slow component		Std-state (A_{stst})
	Speed τ(r)	Decay A_r	Speed τ(s)	Decay A_s	
Frequency dev. (0.84)	7.8 (3.9-12.2)	0.3 (0.2-0.4)	74.0 (59.4-88.5)	0.4 (0.3-0.4)	0.14 (0.13-0.15)
Double dev. (0.58)	0.9 * (0.5-1.2)	1.4 * (0.7-2.2)	80.9 (58.1-103)	0.1 * (0.2-0.3)	0.09 * (0.08-0.10)
Intensity dev. (0.66)	0.8 * (0.5-1.1)	2.0 * (1.0-3.0)	45.6 (33.1-58.1)	0.2 * (0.1-0.2)	0.10 * (0.09-0.11)

Non-monotonic neurons also produce adaptation through high intensity sounds

Next, we also tested if non-monotonic IC neurons with SSA are able to maintain their responsiveness to low intensity sounds regardless of the intensity of the conditioner tone. In order to do that, SSA neurons were classified using the monotonicity index (MI: de la Rocha et al., 2008) and divided into monotonic

(MI≥0.75) and non-monotonic neurons (MI<0.75). If non-monotonic IC neurons maintain responsiveness to low intensity sounds, the overall NIA level for the responses to the low intensity deviant in the non-monotonic neurons would be larger than the NIA for the same condition in the monotonic ones. We tested this possibility at all the frequency (Δf=0, Δf=0.04, Δf=0.10 and Δf=0.37) and intensity contrasts (Δi=10, Δi=20-30 and Δi=40-50 dB) used before. Neither of the conditions showed any differences in the NIA of the responses to the deviant between the monotonic and the non-monotonic neurons (Mann-Whitney rank sum test, p>0.1 in all the cases but Δf=0.37 at Δi=30, where p=0.016).

The width of the frequency channel is frequency and intensity dependent

Considering that SSA is frequency and intensity dependent (Duque et al., 2012), we also wished to check if this dependence affects the width of the frequency channel. We analyzed if the frequency channels were wider at low- than at high frequencies and if the frequency channels that code for higher intensities presented also wider bandwidths than the ones than also code for lower intensities. To do so, we only considered the neurons with significant SSA (CSI≥0.18) and looked for any correlation between the frequency and/or the intensity of the probe sound with the NIA values for the deviant response when the conditioner was presented at a fixed intensity contrast (Δi=30) at different frequency contrasts (Δf=0.04, 0.1 and 0.37, Figure 7A). The results demonstrate that the NIA values for the deviant response when the conditioner was at a Δi=30 with a Δf=0.04 did not present a significant correlation with the frequency or the intensity of the probe sound (Spearman rank order correlation, p=0.38 and p=0.89, respectively). The same was observed when the conditioner was at a Δi=30 with a Δf=0.37 (Spearman rank order correlation, p=0.77 and p=0.22, respectively). As expected, at a Δf=0.04 the NIA values were close to 0 regardless of the frequency and the intensity of the probe sound, while at a Δf=0.37 the values were high regardless of the frequency and the intensity of the probe. Interestingly, the trend disappeared when we analyzed the data at Δf=0.1: the width of the frequency channels had a clear dependence on the frequency and the intensity of the probe sound (Spearman rank order correlation, r_{freq}=0.239 r_{int}=-0.26; p≤0.05 in both cases; Figure 7C-D, respectively). Thus, while the frequency channel seems to generally cover the 0.057 octaves range implicit in the 0.04 frequency contrast (regardless of the frequency and the intensity of the probe sound), the 0.141 octaves range embedded in the Δf=0.1 can lie either inside

(at low frequencies and higher intensities) or outside the frequency channel (at high frequencies and lower intensities, Figure 7A). On the other hand, the 0.526 octaves range related with a Δf=0.37 usually falls out the frequency channel, no matter what the frequency or the intensity of the probe sound is.

Neurons with high SSA levels have narrow frequency channels

In order to understand the shape of those frequency channels, we establish a *rapid adaptation paradigm* (RAP; see Methods and Figure 1C), that allows to compare the FRA and the area of frequencies and intensities capable of generating adaptation to the low intensity probe sound. Figure 8A shows an example of the FRA (left chart) and the area of suppression obtained with the RAP (upper right chart), where the probe sound is represented by a black dot over the charts. To confirm that the adaptation observed in the RAP is unrelated to forward suppression (Nelson et al., 2009), a two-tone protocol was also tested in 7 of these neurons (in such protocol 2 sounds were presented and the probe sound was immediately presented after the conditioner, with a conditioner-probe delay of 0 ms). The area of suppression of the two-tone protocol usually covered the whole FRA (Figure 8A, bottom right chart) and even a low intensity conditioner produced suppression of the probe sound. Thus, the areas of suppression were different between the RAP and the two-tone protocol, proving to be independent processes.

Thirty-three neurons were recorded with the RAP. Neurons with high levels of SSA (Figure 8B-C) showed a narrow frequency channel, while neurons with lower levels presented a broad frequency channel (Figure 8D-E). In order to quantify such differences, we calculated ratio between the bandwidth of the frequency channel and the FRA (Figure 8F-G). A simple regression of the bandwidth at 10 and 30 dB above the probe sound show that the neurons with high frequency SSA sensitivity have narrower frequency channels (Figure 8F). With the aim of quantify this trend, we divided the neurons evaluated with the RAP in two groups, regarding its SSA sensitivity. Thus, when we compared both populations we found that the frequency channel in the neurons with high frequency SSA sensitivity (n=21) barely covered a quarter of the FRA at 10 and 30 dB reTh, while the frequency channels found in the neurons with low frequency SSA sensitivity were broader (Figure 8G Mann-Whitney rank sum test, $p<0.05$ at both 10 and 30 dB reTh). Last, the bandwidth ratio

demonstrated a narrow frequency channel in the high SSA neurons compared with the neurons that showed low SSA.

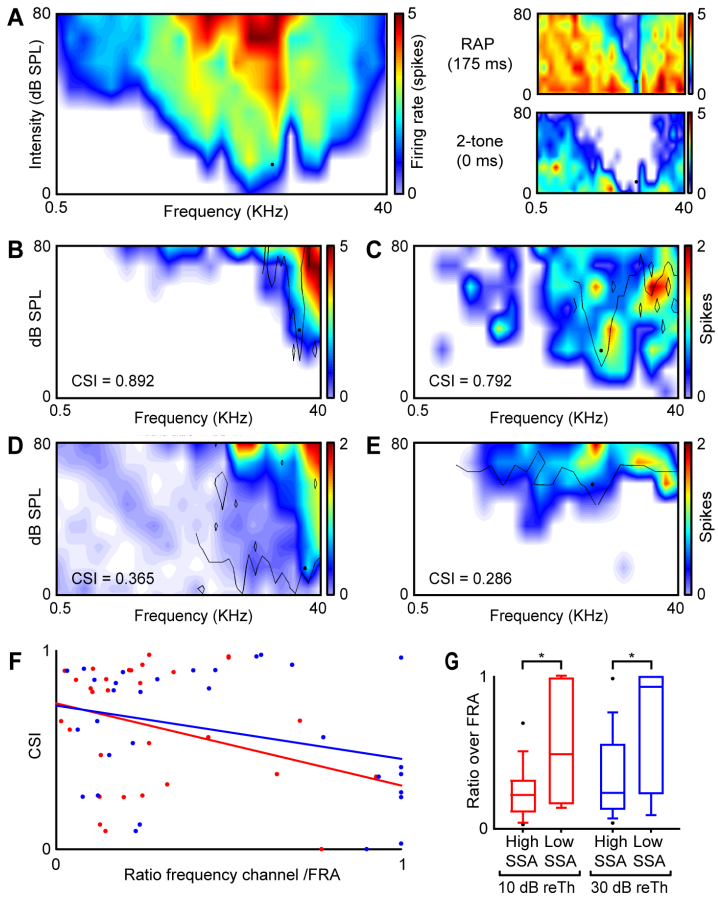

Figure 8. Rapid adaptation paradigm. A. A FRA of an IC neuron is shown in the left panel. The probe sound used in the RAP protocol is represented as a black dot over the FRA. In the right panels, responses to the probe sound are shown at a conditioner-probe delay of 1) 175 ms (RAP protocol; upper right, adaptive processes) and 2) 0 ms (2-tones suppression; bottom right, forward suppression). The area of suppression obtained in the RAP protocol is defined as *frequency channel*. **B-C.** FRAs of two neurons with high frequency-deviant SSA with its corresponding frequency channels. **D-E.** FRAs of two neurons with low frequency deviant SSA and its corresponding frequency channels. Note that the width of the frequency channels is larger in **D-E** than in **B-C**. **F.** Correlation between the proportion of the FRA covered by the frequency channels against the CSI at 10- (red lines and dots) and 30 dB (blue lines and dots) over threshold. **G.** Proportion of the FRA covered by the frequency channels computed in the neurons with high- and low frequency deviant SSA. The bandwidth of the frequency channels at both 10 and 30 dB over threshold cover less frequency range of the FRA in the neurons with high frequency deviant SSA.

DISCUSSION

Our results demonstrate that neither monotonic nor non-monotonic IC neurons show SSA for purely intensity deviant sounds, as they are not able to detect low intensity tones embedded within a sequence of the same tone at higher intensities. Nevertheless, the analysis of the double deviant data shed light on the across-adaptation caused from the high- to the low intensity sounds. Thus, SSA can be elicited if and when the high intensity conditioner sound is outside the frequency channels that code for the probe sound. The width of the channels is frequency- and intensity dependent, and neurons with high frequency SSA sensitivity present narrow frequency channels.

Comparison with previous studies

In the present account we demonstrate that neurons of the IC are sensitive to SSA for high intensity deviant sounds, as in the auditory cortex (Ulanovsky et al., 2003; Farley, 2010) but not to low intensity deviants. In the cortex however, and despite the pattern of neuronal responses reported in these two studies being similar, one study interprets as SSA for low intensity deviants (Ulanovsky et al., 2003) while another did not (Farley et al., 2010). The first claimed that the results were inconsistent with a purely adaptive phenomenon ($SI_{low} + SI_{high} > 0$) while the latter reported gain changes. Our results conform to the gain changes explanation (Sign test for $SI_{low} + SI_{high} = 0$; p=0.392), demonstrating the absence of SSA for low intensity deviant sounds.

Näätänen's seminal paper (1978) demonstrated that MMN could be elicited by intensity increments and posterior works showed it also with intensity decrements (Näätänen et al., 1987, 1989a, 1989b; Paavilainen et al., 1991, 1993). An elegant paper (Jacobsen et al., 2003) demonstrated stimulus-specific MMN responses for both intensity increments and decrements, but they show that the P1-N1 component to the low intensity deviant was similar (or even smaller) to the same tone as standard. P1 and N1 components are attributed to basic auditory perception from the auditory cortex (Hari et al., 1984; Maess et al., 2007) and such reduced response conform to the data presented here. Middle latency responses (Althen et al., 2011) also showed MMN-like responses to intensity decrements between the Na and the Pa components, although the negative deflection observed by these authors (Figure 6C from Althen et al., 2011) could also be reflecting across-adaptation from high to low intensity sounds.

If that is so, intensity coding would be dominated by across-adaptation from high- to low intensities and genuine intensity discrimination (Jacobsen et al., 2003) would be generated only at high order cortical areas. Considering that 1) true intensity SSA neurons should respond better to both low- and high-intensity deviant sounds and that 2) only 4 out of 117 neurons analyzed (3.4%) showed a slightly larger sensitivity to low intensity deviant sounds, we conclude that IC neurons do not present purely intensity SSA.

Frequency channel model in the inferior colliculus

Since inhibition is only playing a key role in modulating SSA but not in its generation (Pérez-González et al., 2012; Duque et al., 2014), a synaptic depression fatigue model (Grill-Spector et al., 2006; Briley and Krumbholz, 2013) has been proposed as the most likely explanation for SSA (Eytan et al., 2003; Mill et al., 2011a, 2011b), although more complex mechanisms may explain it at the cortical level (Taaseh et al., 2011; Hershenhoren et al., 2014). However, the data shown in the present account from the IC perfectly fits this model (Figure 9A). In the frequency domain, as long as the repeated frequency is outside the frequency channel (Figure 9A, diamond) SSA would be present (Figure 9B). In the intensity domain, regardless the intensity of the repeated frequency (Figure 9A, square) across-adaptation from high- to low intensities will always be present (Figure 9C). If we present a high intensity sound with a different frequency (Figure 9A, triangle), SSA would depend on the width of the frequency channel. If the repeated frequency is outside the frequency channel there will be no across-adaptation; but if it is inside the resulting probe response will be reduced (Figure 9D). Interestingly, MMN responses to double deviants did not show additivity (Paavilainen et al., 2001; Wolff and Schröger, 2001) which implies that MMN, as well as SSA, do not process frequency and intensity information independently. Moreover, the analysis of the N1 component provided a similar frequency channel model (Näätänen et al., 1988; Herrmann et al., 2013, 2014), pointing out the similarities between the adaptive processes in SSA and MMN.

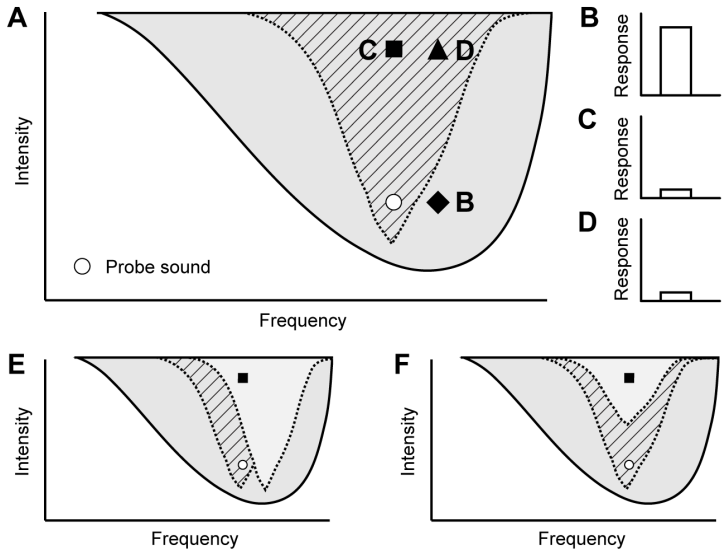

Figure 9. Model of the frequency and intensity dependence of SSA in an IC neuron. A. Schematic FRA showing the response of an IC neuron. The probe sound is represented as a white circle and three different conditioner sounds are also drawn as black figures. The theoretical area of the frequency channel coding for the probe sound is represented as a region with diagonal lines. **B.** Response to the probe sound when the conditioner sound is in B. No cross adaptation is observed. **C.** Response to the probe sound when the conditioner sound is in C. Cross adaptation suppress the response to the probe sound. **D.** Response to the probe sound when the conditioner sound is in D. Cross adaptation could be observed depending on the width of the frequency channel. **E-F.** The reduced SSA observed at high intensities could be due to additional frequency channel that expanded at high intensities (**E**) or to specific high-intensity channels that do not usually show adaptation (**F**).

Neurons with high frequency SSA show narrow frequency channels (Figures 6 and 8). As we have previously demonstrated that frequency SSA neurons present broad FRAs (Duque et al., 2012), it is tempting to speculate that such neurons can integrate more frequency inputs. Moreover, the low levels of frequency SSA observed at high intensities (Duque et al., 2012) may be explained because the frequency channels broaden monotonically with intensity. We also showed that frequency channels are narrower at high frequencies, consequently increasing adaptation at high frequencies (Figure 7C-D), a phenomenon that has been previously observed in the auditory nerve fibers (Westerman and Smith, 1985) and the IC (Figure 5 from Dean et al., 2008; Figure 7C from Duque et al., 2012) and may be related with the great amount of high frequency behaviorally relevant sounds rat usually process.

Forward suppression, SSA and adjustment to sound intensity statistics

The current data support the idea that there is no SSA for intensity deviant sounds because of forward suppression-like phenomena. If that is so, adjustments to sound intensity statistics (Dean et al., 2005) could only be produced from low- to high intensity sounds. At first sight, this does not fit with the data presented by Dean and colleagues (2005) where, at a population level, bimodal stimuli adjust responses to incorporate both low- and high-intensity regions (Dean et al., 2005). Nevertheless, these authors commented that individual neurons did not show any obvious trend to adjust to both low- and high-intensity regions (Figure 4C from Dean et al., 2005).

SSA at the intensity domain greatly resembles forward suppression in the IC (Nelson et al., 2009), but some differences arise when comparing both studies. First, forward suppression would involve inhibitory mechanisms (Nelson et al., 2009), but we have previously demonstrated that SSA is not generated by GABAergic inhibition in both the IC (Pérez-González et al., 2012) and the thalamus (Duque et al., 2014). In fact, as non-monotonic SSA neurons in the IC –generated by GABAergic inhibition (Sivaramakrishnan, et al., 2004; Grimsley et al., 2013)– do not maintain responsiveness to low intensity sounds embedded in a background of loud sounds, inhibitory generation of non-monotonicity in the IC would be a *post hoc* phenomenon independent of the excitatory inputs that generate SSA. Nevertheless, such non-monotonicity could eventually lead to deviant detection at more high-level relay stations of the auditory system, like the auditory cortex (Watkins and Barbour, 2008; 2011a; 2011b). Secondly, forward suppression in the IC is evident up to ~70 ms conditioner-probe delays (Nelson et al., 2009). In the present account, delays of 175 ms were used between the sounds, a condition that in the IC only showed a ~5 dB residual masking (Nelson et al., 2009). Finally, forward suppression experiment were conducted in central nucleus IC-like neurons (Nelson et al., 2009), while our SSA data population is biased to non-lemniscal regions of the IC (Malmierca et al., 2009; Duque et al., 2012; Pérez-González et al., 2012; Ayala et al., 2013).

In contrast, experiments performed in the auditory cortex (Calford and Semple, 1995; Brosch and Schreiner, 1997; Scholl et al., 2008; Scholes et al., 2011) suggest that forward suppression effects with conditioner-probe intervals higher than 100-150 ms are attributable to SSA, probably through synaptic depression (Wehr and

621 Zador, 2005; Scholes et al., 2011). If forward suppression is a merely adaptive process,
622 the absence of intensity SSA would be determined by the overlap in the synapses
623 activated by high- and low intensity sounds (Scholl et al., 2008). Indeed, the dynamics
624 of adaptation for forward suppression, intensity SSA and dynamic range adjustments
625 are virtually identical. The three phenomena seem to all share dual adaptations that
626 comprise 1) an input related mechanism (*i.e.*, synaptic depression) and 2) a gain control
627 mechanism (*i.e.*, inhibition), where the input related component is generally more
628 relevant (SSA: Ulanovsky et al., 2003; Pérez-González et al., 2012; forward
629 suppression: Scholl et al., 2008; dynamic range adjustment: Wen et al., 2009). Such
630 dual adaptation is also reflected in the similar time constants obtained when evaluating
631 the time course of adaptation (Ulanovsky et al., 2004; Dean et al., 2008).

632 In summary, our data indicates that a dynamic range adjustment to intensity
633 (Dean et al., 2005) is passively due to SSA (Condon and Weinberger, 1991; Malone
634 and Semple, 2001; Ulanovsky et al., 2003; Malmierca et al., 2009), a phenomenon
635 present for frequency- but not for intensity-deviant tones and that may provide a likely
636 explanation for central forward suppression in the IC.

REFERENCES

Althen H, Grimm S, Escera C (2011) Fast detection of unexpected sound intensity decrements as revealed by human evoked potentials. PLoS One 6:e28522.

Antunes FM, Malmierca MS (2014) An Overview of Stimulus-Specific Adaptation in the Auditory Thalamus. Brain topography.

Antunes FM, Nelken I, Covey E, Malmierca MS (2010) Stimulus-specific adaptation in the auditory thalamus of the anesthetized rat. PLoS One 5:e14071.

Ayala YA, Malmierca MS (2013) Stimulus-specific adaptation and deviance detection in the inferior colliculus. Front Neural Circuits 6:89.

Ayala YA, Perez-Gonzalez D, Duque D, Nelken I, Malmierca MS (2013) Frequency discrimination and stimulus deviance in the inferior colliculus and cochlear nucleus. Front Neural Circuits 6:119.

Briley PM, Krumbholz K (2013) The specificity of stimulus-specific adaptation in human auditory cortex increases with repeated exposure to the adapting stimulus. J Neurophysiol 110:2679-2688.

Brosch M, Schreiner CE (1997) Time course of forward masking tuning curves in cat primary auditory cortex. J Neurophysiol 77:923-943.

Calford MB, Semple MN (1995) Monaural inhibition in cat auditory cortex. J Neurophysiol 73:1876-1891.

Condon CD, Weinberger NM (1991) Habituation produces frequency-specific plasticity of receptive fields in the auditory cortex. Behavioral neuroscience 105:416-430.

Dahmen JC, Keating P, Nodal FR, Schulz AL, King AJ (2010) Adaptation to stimulus statistics in the perception and neural representation of auditory space. Neuron 66:937-948.

de la Rocha J, Marchetti C, Schiff M, Reyes AD (2008) Linking the response properties of cells in auditory cortex with network architecture: cotuning versus lateral inhibition. J Neurosci 28:9151-9163.

Dean I, Harper NS, McAlpine D (2005) Neural population coding of sound level adapts to stimulus statistics. Nat Neurosci 8:1684-1689.

Dean I, Robinson BL, Harper NS, McAlpine D (2008) Rapid neural adaptation to sound level statistics. J Neurosci 28:6430-6438.

Duque D, Malmierca MS, Caspary DM (2014) Modulation of stimulus-specific adaptation by GABAA receptor activation or blockade in the medial geniculate body of the anaesthetized rat. J Physiol 592:729-743.

Duque D, Perez-Gonzalez D, Ayala YA, Palmer AR, Malmierca MS (2012) Topographic distribution, frequency, and intensity dependence of stimulus-specific adaptation in the inferior colliculus of the rat. J Neurosci 32:17762-17774.

Escera C, Malmierca MS (2013) The auditory novelty system: An attempt to integrate human and animal research. Psychophysiology 51:111-123.

Farley BJ, Quirk MC, Doherty JJ, Christian EP (2010) Stimulus-specific adaptation in auditory cortex is an NMDA-independent process distinct from the sensory novelty encoded by the mismatch negativity. J Neurosci 30:16475-16484.

Faure PA, Fremouw T, Casseday JH, Covey E (2003) Temporal masking reveals properties of sound-evoked inhibition in duration-tuned neurons of the inferior colliculus. J Neurosci 23:3052-3065.

Grill-Spector K, Henson R, Martin A (2006) Repetition and the brain: neural models of stimulus-specific effects. Trends Cogn Sci 10:14-23.

Grimsley CA, Sanchez JT, Sivaramakrishnan S (2013) Midbrain local circuits shape sound intensity codes. Front Neural Circuits 7:174.

Hara K, Harris RA (2002) The anesthetic mechanism of urethane: the effects on neurotransmitter-gated ion channels. Anesth Analg 94:313-318, table of contents.

Hari R, Hamalainen M, Ilmoniemi R, Kaukoranta E, Reinikainen K, Salminen J, Alho K, Naatanen R, Sams M (1984) Responses of the primary auditory cortex to pitch changes in a sequence of tone pips: neuromagnetic recordings in man. Neurosci Lett 50:127-132.

Hernandez O, Espinosa N, Perez-Gonzalez D, Malmierca MS (2005) The inferior colliculus of the rat: a quantitative analysis of monaural frequency response areas. Neuroscience 132:203-217.

Herrmann B, Henry MJ, Obleser J (2013) Frequency-specific adaptation in human auditory cortex depends on the spectral variance in the acoustic stimulation. J Neurophysiol 109:2086-2096.

Herrmann B, Schlichting N, Obleser J (2014) Dynamic range adaptation to spectral stimulus statistics in human auditory cortex. J Neurosci 34:327-331.

Hershenhoren I, Taaseh N, Antunes FM, Nelken I (2014) Intracellular correlates of stimulus-specific adaptation. J Neurosci 34:3303-3319.

Jacobsen T, Horenkamp T, Schroger E (2003) Preattentive memory-based comparison of sound intensity. Audiol Neurootol 8:338-346.

Loewy DH, Campbell KB, de Lugt DR, Elton M, Kok A (2000) The mismatch negativity during natural sleep: intensity deviants. Clin Neurophysiol 111:863-872.

Loftus WC, Malmierca MS, Bishop DC, Oliver DL (2008) The cytoarchitecture of the inferior colliculus revisited: a common organization of the lateral cortex in rat and cat. Neuroscience 154:196-205.

Maess B, Jacobsen T, Schroger E, Friederici AD (2007) Localizing pre-attentive auditory memory-based comparison: magnetic mismatch negativity to pitch change. NeuroImage 37:561-571.

Malmierca M, Ryugo D (2011) Auditory System. In: The Mouse Nervous System 1st Edition, pp 607-645. San Diego, CA: Academic Press.

Malmierca MS, Seip KL, Osen KK (1995) Morphological classification and identification of neurons in the inferior colliculus: a multivariate analysis. Anat Embryol (Berl) 191:343-350.

Malmierca MS, Cristaudo S, Perez-Gonzalez D, Covey E (2009) Stimulus-specific adaptation in the inferior colliculus of the anesthetized rat. J Neurosci 29:5483-5493.

Malmierca MS, Blackstad TW, Osen KK, Karagulle T, Molowny RL (1993) The central nucleus of the inferior colliculus in rat: a Golgi and computer reconstruction study of neuronal and laminar structure. J Comp Neurol 333:1-27.

Malmierca MS, Hernandez O, Falconi A, Lopez-Poveda EA, Merchan M, Rees A (2003) The commissure of the inferior colliculus shapes frequency response areas in rat: an in vivo study using reversible blockade with microinjection of kynurenic acid. Exp Brain Res 153:522-529.

Malone BJ, Semple MN (2001) Effects of auditory stimulus context on the representation of frequency in the gerbil inferior colliculus. J Neurophysiol 86:1113-1130.

Mill R, Coath M, Wennekers T, Denham SL (2011a) Abstract Stimulus-Specific Adaptation Models. Neural Comput.

Mill R, Coath M, Wennekers T, Denham SL (2011b) A neurocomputational model of stimulus-specific adaptation to oddball and Markov sequences. PLoS Comput Biol 7:e1002117.

Näätänen R, Paavilainen P, Reinikainen K (1989a) Do event-related potentials to infrequent decrements in duration of auditory stimuli demonstrate a memory trace in man? Neurosci Lett 107:347-352.

Näätänen R, Paavilainen P, Alho K, Reinikainen K, Sams M (1987) The mismatch negativity to intensity changes in an auditory stimulus sequence. Electroencephalography and clinical neurophysiology Supplement 40:125-131.

Näätänen R, Paavilainen P, Alho K, Reinikainen K, Sams M (1989b) Do event-related potentials reveal the mechanism of the auditory sensory memory in the human brain? Neurosci Lett 98:217-221.

Näätänen R, Sams M, Alho K, Paavilainen P, Reinikainen K, Sokolov EN (1988) Frequency and location specificity of the human vertex N1 wave. Electroencephalogr Clin Neurophysiol 69:523-531.

Näätänen R (1992) Attention and Brain Function. Hillsdale, NJ: Erlbaum.

Näätänen R, Gaillard AW, Mantysalo S (1978) Early selective-attention effect on evoked potential reinterpreted. Acta Psychol (Amst) 42:313-329.

Nelken I (2014) Stimulus-specific adaptation and deviance detection in the auditory system: experiments and models. Biol Cybern.

Nelson PC, Smith ZM, Young ED (2009) Wide-dynamic-range forward suppression in marmoset inferior colliculus neurons is generated centrally and accounts for perceptual masking. J Neurosci 29:2553-2562.

Paavilainen P, Valppu S, Naatanen R (2001) The additivity of the auditory feature analysis in the human brain as indexed by the mismatch negativity: 1+1 approximately 2 but 1+1+1<3. Neurosci Lett 301:179-182.

Paavilainen P, Jiang D, Lavikainen J, Naatanen R (1993) Stimulus duration and the sensory memory trace: an event-related potential study. Biol Psychol 35:139-152.

Paavilainen P, Alho K, Reinikainen K, Sams M, Naatanen R (1991) Right hemisphere dominance of different mismatch negativities. Electroencephalogr Clin Neurophysiol 78:466-479.

Paxinos G, Watson C (2005) The rat brain in stereotaxic coordinates. Burlington: Elsevier-Academic.

Perez-Gonzalez D, Hernandez O, Covey E, Malmierca MS (2012) GABA(A)-Mediated Inhibition Modulates Stimulus-Specific Adaptation in the Inferior Colliculus. PLoS One 7:e34297.

Pérez-González D, Malmierca MS, Covey E (2005) Novelty detector neurons in the mammalian auditory midbrain. Eur J Neurosci 22:2879-2885.

Rabinowitz NC, Willmore BD, Schnupp JW, King AJ (2011) Contrast gain control in auditory cortex. Neuron 70:1178-1191.

Reches A, Gutfreund Y (2008) Stimulus-specific adaptations in the gaze control system of the barn owl. J Neurosci 28:1523-1533.

Scholes C, Palmer AR, Sumner CJ (2011) Forward suppression in the auditory cortex is frequency-specific. Eur J Neurosci.

Schroger E, Wolff C (1996) Mismatch response of the human brain to changes in sound location. Neuroreport 7:3005-3008.

Simpson AJ, Harper NS, Reiss JD, McAlpine D (2014) Selective adaptation to "oddball" sounds by the human auditory system. J Neurosci 34:1963-1969.

Sivaramakrishnan S, Sterbing-D'Angelo SJ, Filipovic B, D'Angelo WR, Oliver DL, Kuwada S (2004) GABA(A) synapses shape neuronal responses to sound intensity in the inferior colliculus. J Neurosci 24:5031-5043.

Taaseh N, Yaron A, Nelken I (2011) Stimulus-specific adaptation and deviance detection in the rat auditory cortex. PLoS One 6:e23369.

Ulanovsky N, Las L, Nelken I (2003) Processing of low-probability sounds by cortical neurons. Nat Neurosci 6:391-398.

Ulanovsky N, Las L, Farkas D, Nelken I (2004) Multiple time scales of adaptation in auditory cortex neurons. J Neurosci 24:10440-10453.

Wark B, Lundstrom BN, Fairhall A (2007) Sensory adaptation. Curr Opin Neurobiol 17:423-429.

Watkins PV, Barbour DL (2008) Specialized neuronal adaptation for preserving input sensitivity. Nat Neurosci 11:1259-1261.

Watkins PV, Barbour DL (2011a) Level-tuned neurons in primary auditory cortex adapt differently to loud versus soft sounds. Cereb Cortex 21:178-190.

Watkins PV, Barbour DL (2011b) Rate-level responses in awake marmoset auditory cortex. Hear Res 275:30-42.

Wehr M, Zador AM (2005) Synaptic mechanisms of forward suppression in rat auditory cortex. Neuron 47:437-445.

Wen B, Wang GI, Dean I, Delgutte B (2009) Dynamic range adaptation to sound level statistics in the auditory nerve. J Neurosci 29:13797-13808.

Wen B, Wang GI, Dean I, Delgutte B (2012) Time course of dynamic range adaptation in the auditory nerve. J Neurophysiol 108:69-82.

Westerman LA, Smith RL (1985) Rapid adaptation depends on the characteristic frequency of auditory nerve fibers. Hear Res 17:197-198.

Wolff C, Schroger E (2001) Human pre-attentive auditory change-detection with single, double, and triple deviations as revealed by mismatch negativity additivity. Neurosci Lett 311:37-40.

Xu X, Yu X, He J, Nelken I (2014) Across-ear stimulus-specific adaptation in the auditory cortex. Front Neural Circuits 8:89.

Yaron A, Hershenhoren I, Nelken I (2012) Sensitivity to complex statistical regularities in rat auditory cortex. Neuron 76:603-615.

Zhou Y, Wang X (2014) Spatially extended forward suppression in primate auditory cortex. Eur J Neurosci 39:919-933.